WATER RESOURCES RESEARCH, VOL. 18, NO. 4, PAGES 865–876, AUGUST 1982

Linear Kernels for Karst Aquifers

SHIRLEY J. DREISS*

Board of Earth Sciences, University of California, Santa Cruz, California 95064

Karst aquifers contain significant water reserves in many parts of the world, but development and management of these reserves is difficult because of the complexity of the aquifers. This paper presents a method of characterizing karst aquifers based on the use of single, linear kernel functions. The kernels are identified with a deconvolution technique proposed by Neuman and de Marsily (1976) by using estimated groundwater recharge during isolated storms as the system input and the rapid storm response of spring flow as the system output. Derived kernels for large springs from data for different storms are similar in shape and time to peak. Average kernels derived from spring flow responses for multiple storms differ in shape for different springs but suggest a regularity in the response of individual springs to precipitation. The derived kernel functions presently cannot be validated because of the use of a scaling factor in the moisture balance for the springs. They can be used, however, to predict the storm response of a spring if the total volume of the rapid spring flow response is known.

INTRODUCTION

Karst aquifers are important sources of groundwater in many parts of the world. However, because the aquifers are generally complex, management of karst groundwater reserves and evaluation of potential contaminant transport is difficult. Commonly, extensive field work and tracer or water quality studies are required to determine pertinent information, such as recharge areas of springs, rate of groundwater movement, and the moisture balance of an aquifer [*Shuster and White,* 1972; *Hanshaw and Back,* 1974; *Atkinson et al.,* 1973; *Back et al.,* 1979]. Although numerical models for flow through porous media have produced useful results in addressing regional water supply problems in finely fractured carbonate aquifers, such models are not useful in well-developed karst terrains because of the complexity of the aquifer systems [*Konikow,* 1976; *Klemt,* 1975].

The hydrologic complexity of a karst aquifer is caused by highly variable recharge conditions and by heterogeneous subsurface flow conditions. Water enters a karst aquifer by infiltration through soils, through pores and fractures in exposed rock, and through solution-enlarged fractures and collapse zones. Once in the aquifer, water travels through an interconnected network of pores, fractures, and solution conduits. In many karst aquifers, part of this groundwater flow feeds into large springs. The discharge hydrographs of these springs respond rapidly to intense, isolated storms in a manner similar to the response of surface runoff to intense storms. In the case of large karst springs, the rapid response is a combined response of flow through fractures, pores, and conduits.

This paper presents a method of characterizing karst aquifers with linear kernel functions. The kernel functions are identified by using the rapid response of spring discharge to isolated storms as the system output and calculated groundwater recharge during the storms as the system input. A linear system identification technique proposed by *Neuman and de Marsily* [1976] for identification of instantaneous unit hydrographs is used to identify the kernel functions.

Justification for the use of a linear systems model for what is recognized to be a nonlinear system is twofold. First, detailed deterministic models of karst groundwater flow currently are not feasible. If, for example, a karst aquifer is envisioned as a matrix of interconnected pores, fractures, and conduits, a physically detailed model of the aquifer would require an understanding of the interaction of the different types of flow as well as extensive and possibly unobtainable data, such as fracture and conduit geometries, locations and amounts of discrete recharge and discharge, and values of hydraulic conductivity and storativity for the porous media. Second, as noted above, the discharge hydrographs of large springs respond to precipitation in a manner similar to that of surface runoff hydrographs. Although surface runoff is known to be controlled by nonlinear processes, linear kernel functions are useful on a practical level. Similarly, kernel functions may be useful in providing information about karst aquifers, even though the kernel functions lump the effects of several complex processes.

SYSTEM CONCEPTUALIZATION

If a system, in this case a karst aquifer, is assumed to act as a single, linear, time-invariant filter, the relationship between a continuous input series and a resulting continuous output series may be described by the convolution integral

$$y(t) = \int_{-\infty}^{\infty} h(t - \tau)\, x(\tau)\, d\tau \qquad (1)$$

where $y(t)$ is the output or spring discharge, $x(\tau)$ is the input or groundwater recharge, $h(t - \tau)$ is the kernel function, t represents time, and τ is the variable of integration. For two isolated, discrete, finite series that are causally related, the convolution relationship can be written as

$$y_i = \Delta t \sum_{j=0}^{i} x_j h_{i-j} \qquad i = 0, 1, 2, \cdots, N \qquad (2)$$

for $N + 1$ sampling intervals of equal length Δt, where y_i represents the mean value of the output during interval i, x_j represents the mean value of the input during interval j, and h_{i-j} represents the mean value of the kernel function during interval $i - j$. If x_j and h_{i-j} are known, y_i can be found

*Formerly with Department of Geology, Stanford University

Paper number 2W0335.
0043-1397/82/002W-0335$01.00

directly by convolution. If x_j and y_i are known, h_{i-j} can be identified by deconvolution.

When a finite, discrete system is not exactly linear or time invariant or when the input and/or output series contain errors, the convolution relationship in (2) becomes

$$y_i = \Delta t \sum_{j=0}^{i} (x_j h_{i-j}) + \varepsilon_i \qquad i = 0, 1, 2, \cdots, N \qquad (3)$$

where ε_i are residual errors. In this case, identification of h_{i-j} is an optimization problem. For example, a kernel might be identified by solving for the values of h_{i-j}, which minimize the sum of the absolute errors $\Sigma|\varepsilon_i|$.

Identification of discrete kernel functions from measured hydrologic data is difficult because of the sensitivity of deconvolution to inaccuracies in the data or to nonlinearities in the system. As noted by *Eagleson* [1966], *Blank et al.* [1971], and others, small data errors can cause large oscillations in identified kernel functions. In hydrologic studies this instability has been treated by smoothing or filtering either the data or the kernel functions [*Emsellem and de Marsily*, 1969; *Neuman and de Marsily*, 1976].

Several previous studies have identified kernel functions from precipitation and karst spring flow data. *Knisel* [1972] used several deconvolution techniques in comparing kernel functions identified for single, isolated storms. Although the identified kernels were oscillatory and physically unrealistic, Knisel's study demonstrated the feasibility of identifying kernel functions from karst spring flow data. *Poitrinal and de Marsily* [1973] and *Poitrinal* [1974] derived stable, physically reasonable, kernel functions for adjusted long-term precipitation and spring discharge records by using a deconvolution technique described in their paper. The resulting kernels, identified from 3 years of data sampled at 5-day intervals, have memories of 2 to 3 months and reproduce the general trend of spring discharge records. Because of the length of the sampling interval, these kernels did not describe rapid, short-term, spring flow responses, such as those addressed in this paper.

Field Site Description

Spring discharge records for four gaged springs in southeastern Missouri were used in the kernel function identifications. The Missouri area was chosen as a study site because of the availability of hydrologic data and the small amount of human interference. The area covers about 7380 km^2 of Mark Twain National Forest, is densely vegetated, and is not disturbed by urbanization or large groundwater pumpage. Continuous or consistently sampled discharge records are available for the largest springs in the region, and previous water chemistry and tracing studies give some information about the recharge areas of these springs. As shown in Figure 1, there are 11 precipitation stations, eight river discharge gaging stations, and four spring flow gaging stations in the area. Two of the springs, Big Spring and Greer Spring, are monitored by the U.S. Geological Survey with continuous stage recorders. Two other springs, Alley Spring and Round Spring, are measured daily with nonrecording gages.

Rates and pathways of tracer movement provide convincing evidence of the complexity of groundwater movement. The results of a tracing study by *Aley* [1975] demonstrate that groundwater travels to large springs over distances as great as 65 km at average rates of up to 342 km/h (Figure 2). The paths go under surface channels and drainage divides, and they overlap other tracer paths to different springs.

The four gaged springs have individual average daily flow rates of 1.1 to 12 m^3/s and together supply about 25% of the total surface runoff that leaves the study area. Figure 3 is an example of the response of the discharge of Big Spring and the Current River to an isolated storm. For this example and, in general, for other storm responses, peak discharge of the springs and the river occur within a 1-day time interval. Spring flow responses recede more gradually than river discharge responses, however.

It is difficult to describe accurately patterns of groundwater circulation or to define the recharge areas of the springs. The study area is underlain by nearly horizontal, cherty, massively bedded dolomites of the Gasconade, Eminence, and Potosi formations. These formations appear to act as a single, semiconfined aquifer. The aquifer system is recharged rapidly through sinkholes and disappearing streams in the uplands and through collapse zones and swallow holes along river and stream channels. After a storm, rapid groundwater recharge and drainage occur primarily in interconnected solution conduits. Slow drainage, which establishes the base flow of the springs, is probably due to the gradual draining of a large volume of storage in smaller fractures and conduits and in pores.

Method of Kernel Function Identification

The identification of kernel functions for karst springs is ill posed and difficult. Two major problems are encountered in the derivation of kernel functions for karst springs from field data. The first is the basic instability of the deconvolution process. If a smooth, physically meaningful kernel function is desired, deconvolution involves the identification of a plausible kernel that accurately reproduces the system response. Both the smoothness and shape of the kernel function and the accuracy of system response prediction must be considered in the kernel function derivation.

A second difficulty arises from the large number of assumptions that must be made about the hydrology of a karst spring system in order to estimate the input and output series for the deconvolution. For example, to calculate the precipitation that contributes to a particular storm response, the recharge area of each spring must be known. Similarly, soil moisture conditions must be assumed in order to estimate the amount of precipitation lost to soil moisture recharge. The accuracy with which these basic hydrologic assumptions can be made determines, to a large extent, the usefulness of the kernel functions.

Parametric Programing Deconvolution Technique

The deconvolution method used in this study has been described in detail by *Neuman and de Marsily* [1976]. The technique uses linear programing to identify discrete kernel functions that optimally reproduce system responses. Smoothness of the derived kernels is controlled parametrically by using a smoothness criterion defined as the sum of the third differences of the discrete kernel function. Thus a sequence of kernel functions is defined, representing a tradeoff between smoothness and predictive accuracy.

A kernel function is identified by minimizing a functional J_c, defined as the sum of the slack variables u_n and v_n, where either u_n or v_n is always zero:

$$\min J_c = \sum_{n=1}^{N} (u_n + v_n) \tag{4}$$

under the constraints

$$\Delta t \sum_{j=n+1-M}^{n} h_{n+1-j} x_j - y_n + u_n - v_n = 0 \tag{5}$$

where $u_n \geq 0$, $v_n \geq 0$, and $n = 1, 2, \cdots, N$

$$\sum_{k=1}^{M} h_k \leq C \tag{6}$$

where $y_0 = x_0 = h_0 = 0$, the maximum memory length of the system is $M\Delta t$, and C is the maximum area under the kernel function. To facilitate comparison of the derived kernels, C was assigned a value of unity. The identified kernels are, therefore, analogous to instantaneous unit hydrographs.

The functional J_c is an error criterion that can be used to define the predictive accuracy of the deconvolution. Predictive accuracy, in this case, refers to the ability of a kernel function to reproduce the springflow response from which it was derived. The value of J_c is the sum of the absolute differences between the observed output and the output predicted by convolution of the input series with the derived kernel.

The smoothness of the kernel function is described by the sum of its third differences with respect to time and repre-

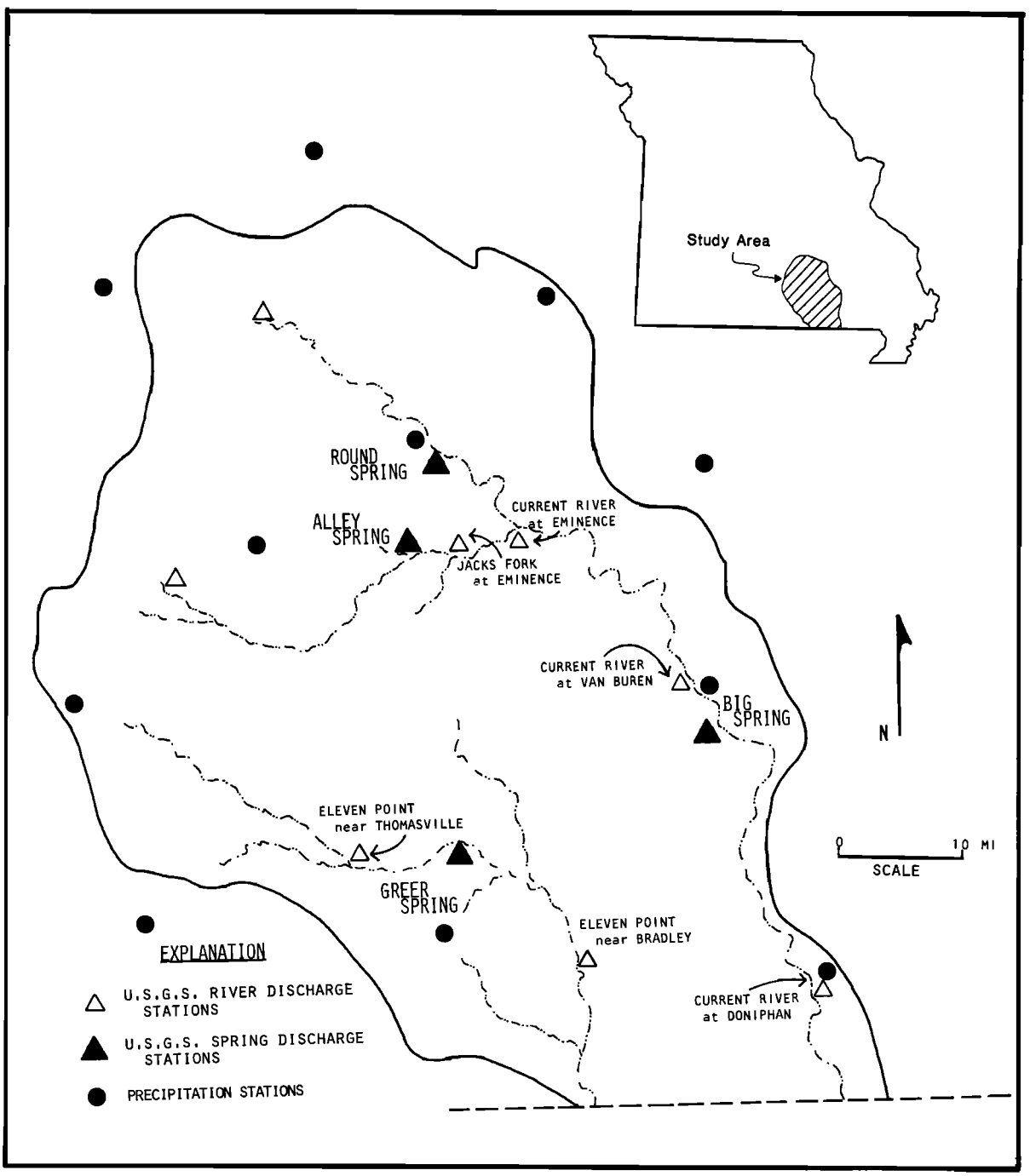

Fig. 1. Location map of data stations in the southeastern Missouri study area.

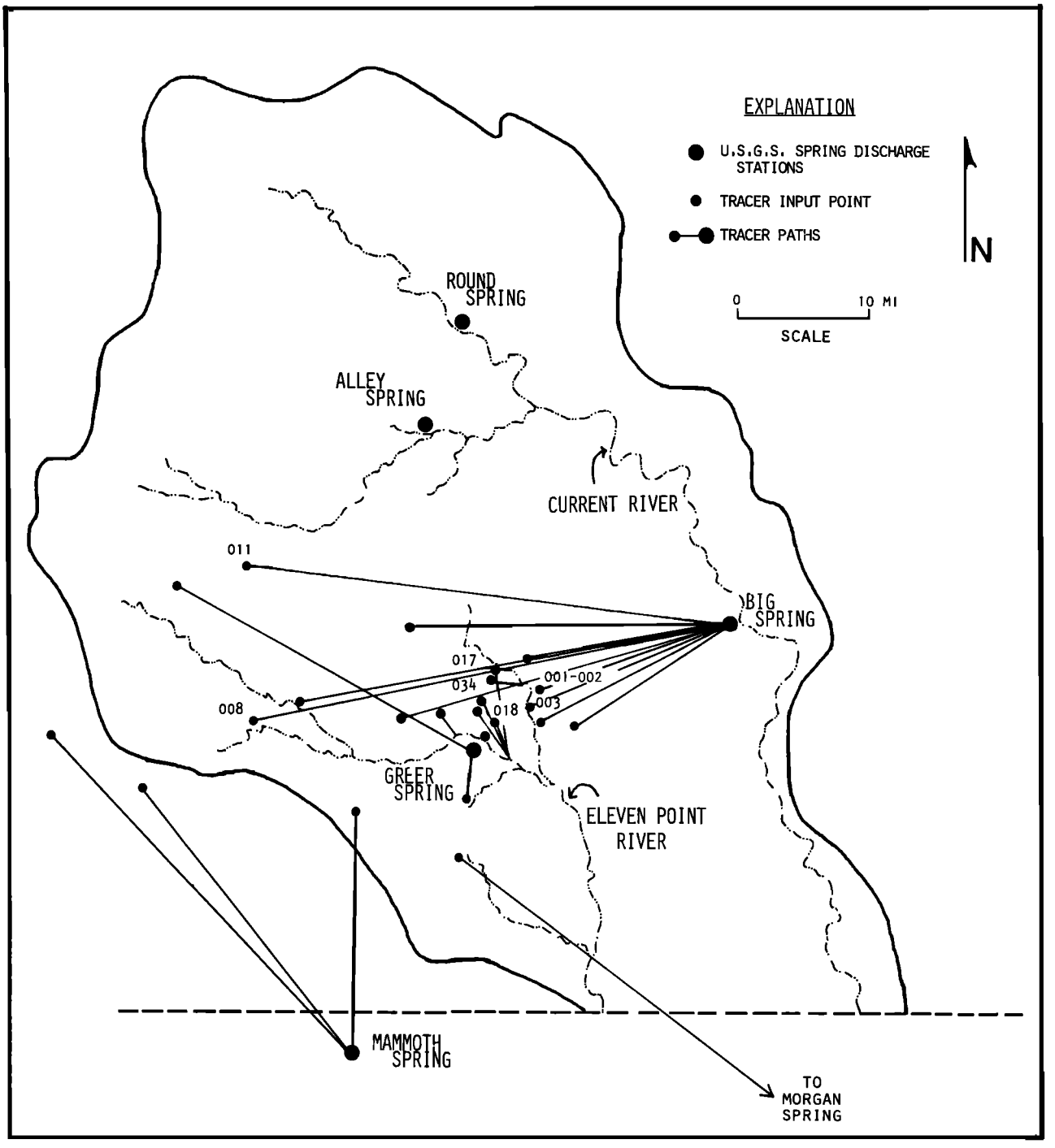

Fig. 2. Paths of tracer movement (adapted from *Aley* [1975]).

sented by the functional J_p, where

$$J_p = \sum_{m=1}^{M-2} (r_m + s_m) \tag{7}$$

and

$$h_{m-1} - 3h_m + 3h_{m+1} - h_{m+2} + r_m - s_m = 0 \tag{8}$$

where $r_m \geq 0$, $s_m \geq 0$, and $m = 1, 2, \ldots, M-2$. The variables r_m and s_m are used to keep the smoothness criterion positive and either r_m or s_m is always zero.

In the parametric programing formulation the functional J_p is constrained by using a parameter θ:

$$J_p \leq \theta \qquad \theta \geq 0 \tag{9}$$

where θ is varied between given limits. Specification of the value of θ in (9) sets an upper limit on the rate of change of curvature of the derived kernel and hence its smoothness.

The linear programing problem defined by (4) through (9) is repetitively solved for sequential values of θ over a specified range. The resulting pairs of values of J_c and J_p for each value of θ form a bicriterion curve where each point on the curve corresponds to a kernel function solution (Figure 4). Because the smoothness criterion J_p is defined by the rate of change of the curvature of the kernel, the form of the bicriterion curve varies with the shape of the derived kernel

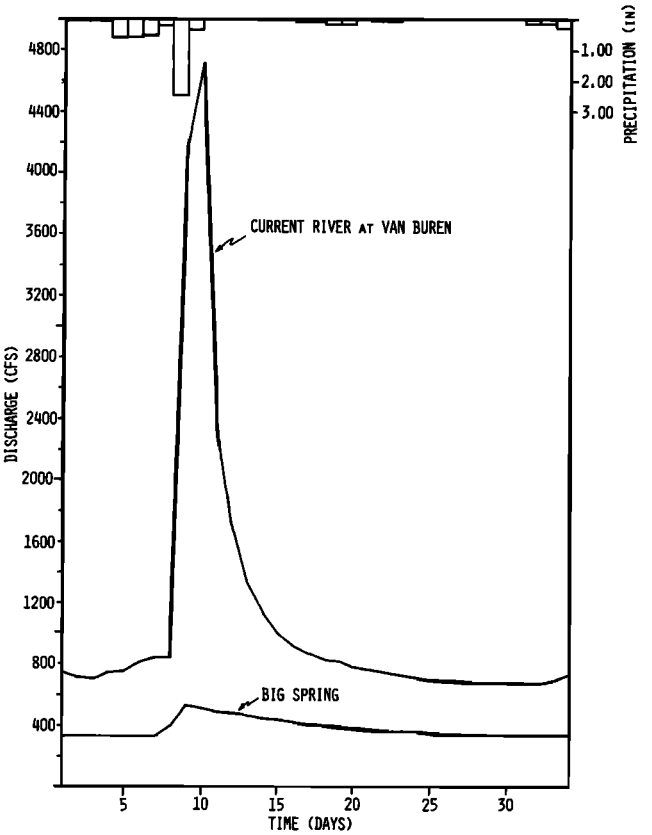

Fig. 3. Response of the discharge of the Current River and Big Spring to August 1970 storm.

as well as with high-frequency oscillations caused by data noise. As J_p increases along the bicriterion curve, the kernel functions become less smooth and the peaks of the kernel functions become sharper (Figures 4 and 5). Typically, high-frequency oscillations begin to develop in the solutions near the break in the slope of the bicriterion curve. As observed by others for surface runoff kernels, these high-frequency oscillations occur at the Nyquist frequency with a period of $2\Delta t$ where Δt is the length of the sampling interval [*Blank et al.*, 1971].

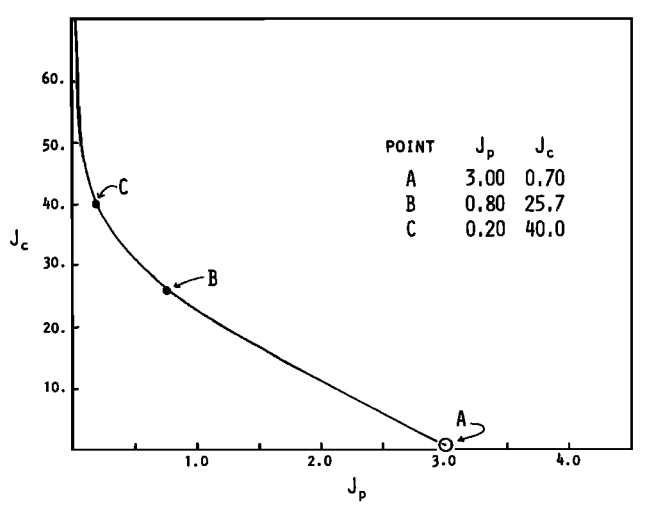

Fig. 4. Bicriterion curve for response of Big Spring to October 1967 storm. J_c is the error functional and J_p is the smoothness functional.

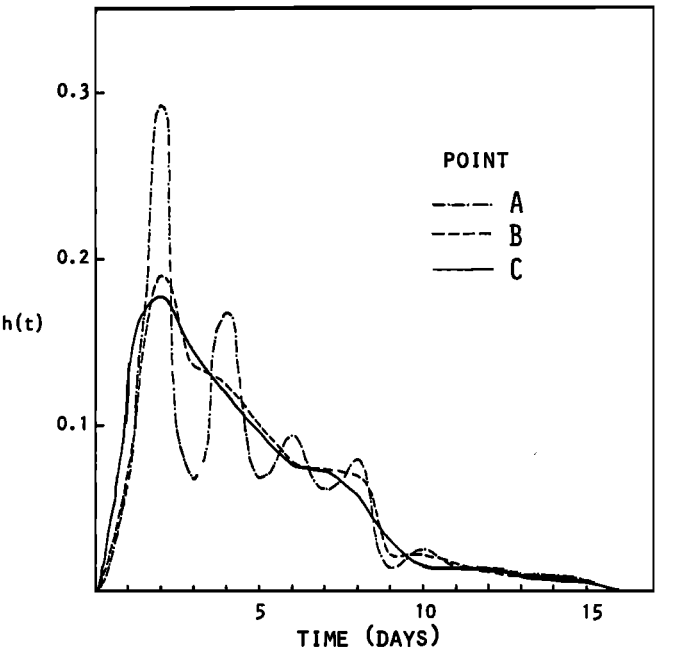

Fig. 5. Alternate kernel functions for response of Big Spring to October 1967 storm for points on the bicriterion curve shown in Figure 4.

The distinctiveness of the break in slope of the bicriterion curve and the way in which the kernel function shapes change along the curve differ for each storm and spring. Hence the decision of where the best solution lies must be made independently for each bicriterion curve. When the bicriterion curve is steep, with only a gentle break in slope, such as the curve in Figure 6, increasing values of J_p yield smooth kernel functions with increasing peaks. Eventually, as J_p is increased further, high-frequency oscillations develop in the solution, as shown in Figure 7. When the bicriterion curves have a sharper break in slope, such as the curve in Figure 4, the kernel solutions have a more complex shape and may have more than one peak. High-frequency oscillations also develop in these solutions as J_p increases. The complex shapes of the functions usually reflect either multiple events in the precipitation records or anomalous discharge measurements.

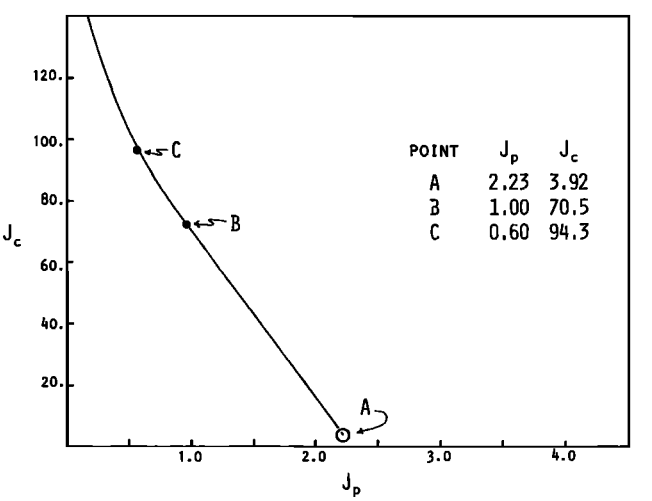

Fig. 6. Bicriterion curve for response of Big Spring to February 1965 storm.

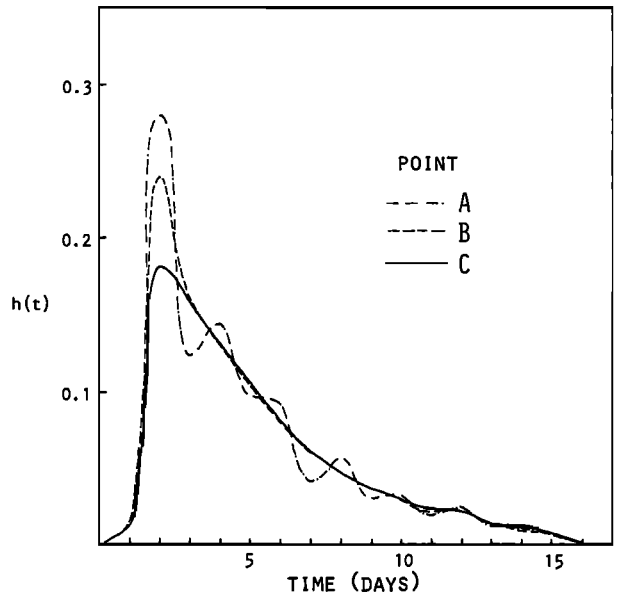

Fig. 7. Alternate kernel functions for the response of Big Spring to February 1965 storm.

The selection of particular solutions from the bicriterion curve is a subjective choice. In this study a kernel function solution usually was chosen at a point just to the right of the region of maximum curvature on the bicriterion curve. For example, in Figures 4 and 6, the kernel functions corresponding to point B on each curve would be used. At Point B, the kernels have been smoothed enough to remove most of the short-period oscillations, and the value of the error functional J_c is still relatively low.

Kernel functions were derived for the response of the four gaged springs by using data from 12 storms. In about half of the kernel derivations, no smoothing was required to define plausible kernel functions. For these solutions the kernel functions with the minimum optimal J_c were used. For the remaining cases, smooth kernels were chosen, using the bicriterion curve.

Estimation of Rapid Groundwater Recharge and Direct Storm Response

In order to estimate the input and output series for the kernel identification, rapid groundwater recharge must be defined from measured precipitation records, and the direct storm response of a spring must be defined from the total measured spring flow storm response. Estimation of the rapid groundwater recharge requires computation of a spatially averaged precipitation record, subtraction of evapotranspiration and soil moisture losses from the average precipitation to define an excess precipitation, and adjustment of the excess precipitation series so that the volume of groundwater recharge is equal to the volume of direct storm response. To compute the direct storm response of a spring, the base flow or slow drainage portion of the spring discharge is separated from the total storm response of the spring.

Spatially averaged precipitation. An average precipitation was estimated for each storm by using Thiessen polygons over an assumed recharge area for each spring. The spring recharge areas were defined from tracing information, topography, the size of the springs, and the general direction of groundwater flow. Since the location and size of the recharge area affect the estimated average precipitation, the shape of the derived kernel and its predictive accuracy are sensitive to the accuracy of the recharge area location.

The sensitivity of derived kernels to the assumed spring recharge area varies greatly for individual storms and depends on the areal distribution of precipitation. Figures 8 and 9 illustrate an example of this sensitivity. The February 1965 storm is an isolated, localized storm which moved from south to north across the study area. Three areas were used to generate spatially averaged precipitation: the total study area, area 1; the most plausible spring recharge area, area 2; and a third area, area 3, which might be proposed if tracer data were not available. The use of area 2 produced a kernel function with the lowest predictive error and the most physically realistic shape. The kernel function for area 1 had less curvature and a higher percent error than the area 2 kernel function. This percent error is the value of J_c expressed as a percentage of the total volume of observed outflow. The derived kernel for area 3 also had a higher percent error than the area 2 kernel and had a time to peak that was shifted in relation to the times to peak of the other kernels.

The shift in the peak of the area 3 kernel is clearly related to the location of the alternate recharge areas and the precipitation pattern of the February 1965 storm. However, a loss of predictive accuracy or a shift in kernel function shape was not observed for all storms [*Dreiss*, 1979]. If precipitation was evenly distributed over a large area for the duration of the storm, derived kernels for different assumed recharge areas were indistinguishable.

Excess precipitation. The daily excess precipitation available for surface runoff and groundwater recharge was calculated by subtracting from the average precipitation the moisture losses caused by evapotranspiration and the changes in soil moisture storage calculated by the moisture balance method of *Thornthwaite and Mather* [1957]. With this method, precipitation not lost to evapotranspiration is assumed to enter the soil instantaneously until the soil moisture storage is filled. The rate at which moisture is withdrawn from the soil by evapotranspiration is taken from soil moisture retention tables by assuming a particular initial soil moisture condition at the beginning of the storm and a value of moisture-holding capacity for the soils. The excess precipitation available for surface runoff and groundwater recharge is the moisture that is left after evapotranspiration and after the soil-moisture-holding capacity is reached.

For this study, initial soil moisture conditions for daily moisture balance calculations were taken from a monthly moisture balance for each year. The soil-moisture-holding capacity was estimated from Missouri soil survey data and from values suggested by *Thornthwaite and Mather* [1957].

Both the assumed soil-moisture-holding capacity and the initial soil moisture conditions affect the amount and temporal distribution of the calculated excess precipitation and, thus, the shape and predictive accuracy of the derived kernels. The major factor that determines the degree to which a storm response is sensitive to initial soil moisture conditions is the length of time between the first day of the moisture balance calculation and the first day of the storm response. Since the effect of variations in the initial conditions are damped by precipitation and evapotranspiration that occur during the period between the specification of the

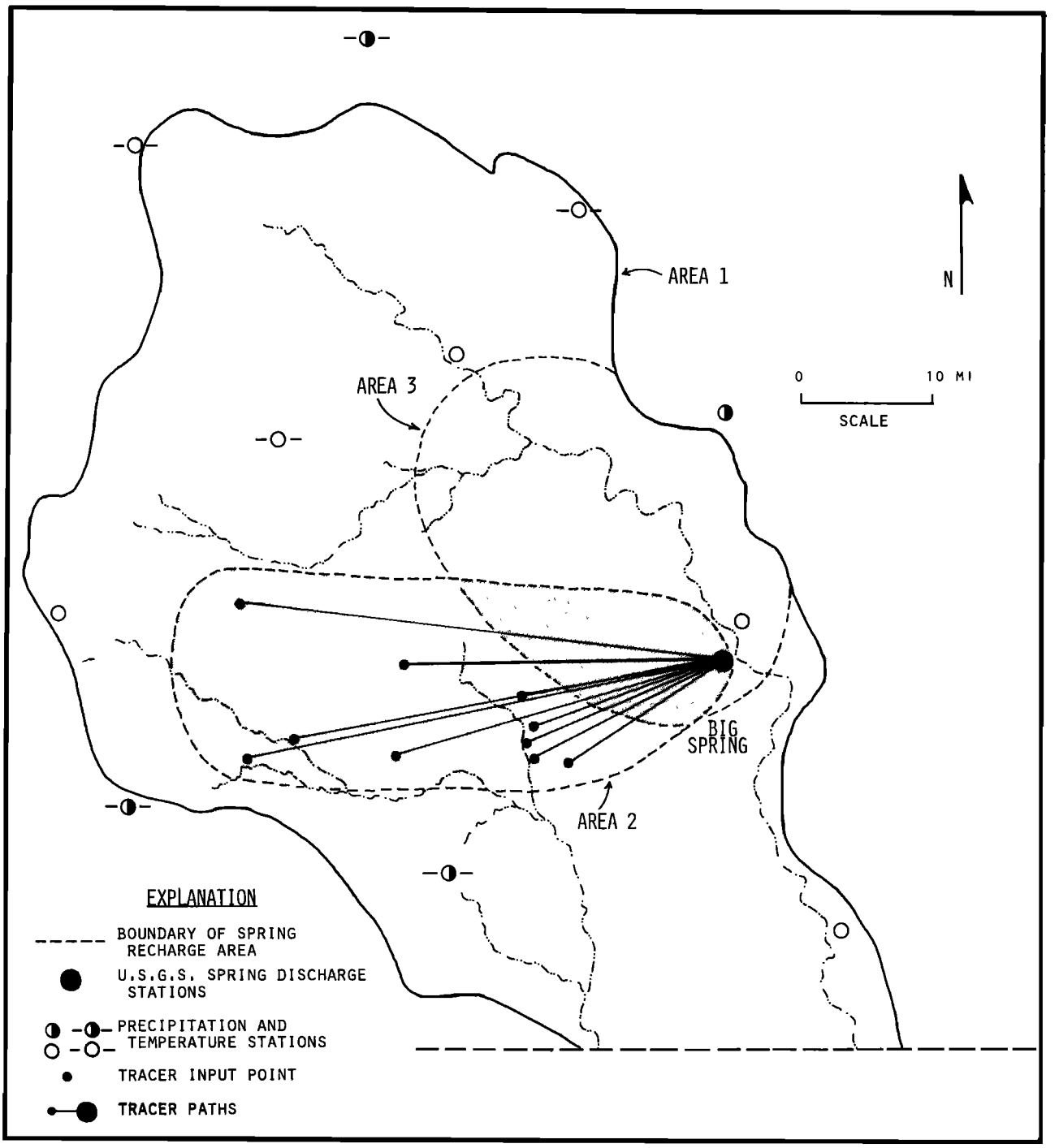

Fig. 8. Alternate recharge areas for Big Spring.

initial conditions and the storm initiation, the exact length of time required for kernels to become insensitive to the initial moisture conditions depends on the pattern and amount of evapotranspiration and precipitation before each storm. For the storms considered here, variations in the initial soil moisture condition did not affect the kernel derivation if the initial conditions were specified at least a month before the storm.

To demonstrate the sensitivity of derived kernels to variations in the values of soil-moisture-holding capacity, kernels were derived for Big Spring for three storms for a range of values of moisture-holding capacity. For each moisture-holding capacity a new monthly moisture balance was computed in order to estimate the proper initial moisture conditions. The effects of changes in the moisture-holding capacity can be seen in the shape and variability of the kernel functions, in the shape of the bicriterion curves for the kernels, and in the predictive accuracy of the kernels.

Figures 10 and 11 show variations in the shapes of derived kernel functions and bicriterion curves for different values of moisture-holding capacity for one of the test storms. The kernel functions have not been smoothed and, therefore, are the solutions for the minimum value of the error criterion J_c. In the example in Figure 10 the kernel derived for a

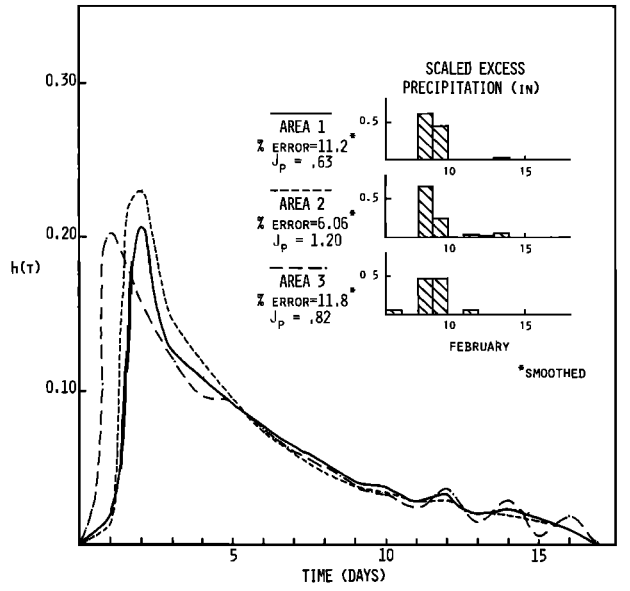

Fig. 9. Derived kernel functions for alternate recharge areas, Big Spring, February 1965 storm.

moisture-holding capacity of 5.1 cm (2 in.) is representative of kernels for moisture-holding capacities between 2.5 and 7.6 cm (1 and 3 in.), with only slight variations in the peak regions. If the moisture-holding capacity is below this range, in this case zero, the kernel rises to a higher peak, the recession limb of the kernel is elevated, and the base length is shorter. Above the 2.5- to 7.6-cm (1- to 3-in.) range, as the holding capacity increases to 10.1 cm (4 in.), the kernel becomes oscillatory. A further increase to 12.7 or 15.2 cm (5 or 6 in.) causes the peaks of the kernels to decrease significantly and to shift forward 1 day in time. The behavior of the kernels for this particular storm is typical of the behavior of the kernels for the other two test storms.

The changes in the kernel functions are reflected in the bicriterion curves for the kernels. The shape of the curves, the minimum values of the error criterion J_c, and the optimal values of the smoothness criterion J_p change with changes in the moisture-holding capacity. As an example, Figure 11 shows the bicriterion curves for the kernel functions in Figure 10. The minimum value of J_c is smallest, i.e., the predictive accuracy is greatest, for holding capacities of 2.5 to 7.6 cm (1 to 3 in.). If the holding capacity is decreased to zero or increased above 7.6 cm (3 in.), the minimum value of J_c increases. Thus, for this example, unsmoothed kernels derived from moisture-holding capacities in the range of 2.5 to 7.6 cm (1 to 3 in.) have the greatest predictive accuracy.

The maximum value of the smoothness criterion J_p is the value of J_p corresponding to the minimum value of J_c. The maximum J_p increases slightly as the moisture-holding capacity is increased from 2.5 to 7.6 cm (1 to 3 in.) and reflects the increase in peakedness in the derived kernel functions. For a holding capacity of 10.1 cm (4 in.) the derived kernel is oscillatory, and J_p is much larger than for other holding capacities. The slope of the lower part of the bicriterion curve is relatively flat, indicating that the derived kernel can be smoothed significantly without introducing large errors in predictive accuracy. Smoothing of the kernels for a moisture-holding capacity of 10.1 cm (4 in.) does not alter its predictive accuracy in relation to the accuracy of the unsmoothed kernels for the other moisture-holding capacities, although smoothing of the kernels for any of the other moisture-holding capacities will reorder their relative accuracy. As the holding capacity is increased further, to 12.7 or 15.2 cm (5 or 6 in.), the value of J_p decreases as the kernel functions change greatly in shape and no longer oscillate.

Figure 12 presents the minimum predictive error for the derived kernels as a function of the moisture-holding capacity for three storms, including the July 1972 storm. For each of the storms the minimum predictive error is lowest for moisture-holding capacities between 2.5 and 7.6 cm (1 and 3 in.). Also, in this range, the minimum predictive error does not change rapidly with changes in the moisture-holding capacity. If the moisture-holding capacity is out of this range, the minimum predictive error increases rapidly.

Soil survey data and values suggested by *Thornthwaite and Mather* [1957] indicate that the soil-moisture-holding capacity of the Missouri soils is probably in the range of 7.6 to 15.2 cm (3 to 6 in.). The moisture-holding capacity values yielding a small minimum predictive error fall at the lower limit of this range. For this reason, a moisture-holding capacity of 7.6 cm (3 in.) was used for the kernel identifications. *Dreiss* [1979] demonstrated that this value is consistent with an overall moisture balance of the study area.

Direct storm response. For a single storm record, the

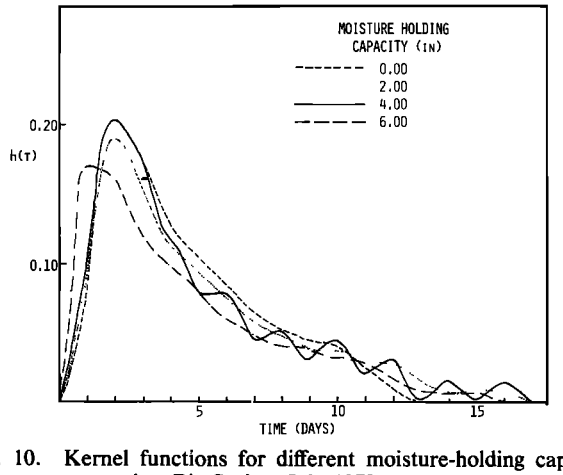

Fig. 10. Kernel functions for different moisture-holding capacities, Big Spring, July 1972 storm.

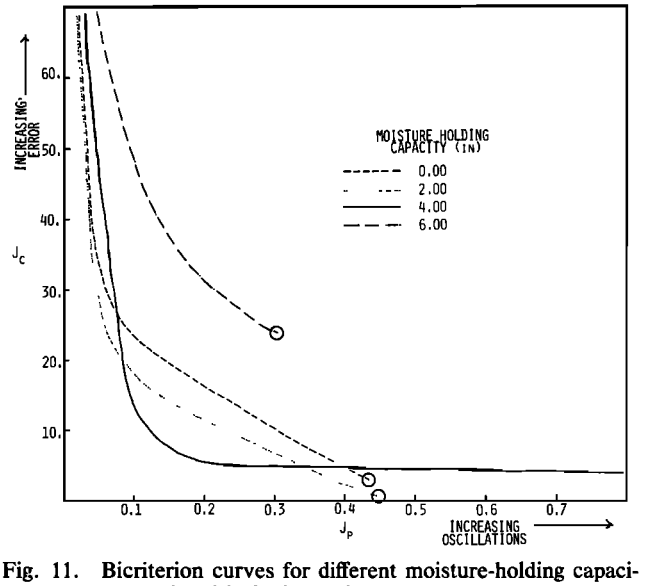

Fig. 11. Bicriterion curves for different moisture-holding capacities, Big Spring, July 1972 storm.

derived kernel function should represent only the rapid response of the aquifer and not gradual groundwater drainage or base flow to the spring from previous precipitation events. In order to isolate the rapid spring response to a particular storm the portion of the springflow from slow drainage was subtracted form the total springflow by drawing a straight line from the point of rise on the hydrograph to a point on the recession limb. In practice the volume of base flow estimated by this straight-line separation is not significantly different from other base flow separation methods. Most of the storms selected for this study occur during times of relatively low flow, when the base flow of the springs is nearly constant and extension of the recession or initial base flow slope makes little difference in the computed direct response.

The base flow separation requires the choice of an endpoint on the recession limb of the storm response curve. This point determines the total response length of the storm and controls the base length of the kernel function. In order to determine this point consistently, each of the springs was assumed to have a constant maximum memory length (the base length of the kernel function), which was estimated from long-duration storm responses. As long as this memory length was large enough to reproduce the long-duration storm responses, the choice of a particular memory length did not significantly affect the shape or predictive ability of the kernels.

A memory length of 16 days was used in most of the kernel derivations. The end of a storm response, therefore, is the point on the storm recession curve 16 days after the last excess precipitation. If an observed storm response length is shorter than 16 days, the last values of the output series are zeros, and the apparent memory length of the derived kernel is shorter than 16 days.

Scaling factor. As defined above, the volume of excess precipitation estimated with the moisture balance is much greater than the volume of the storm response of a spring because the computed excess precipitation includes surface runoff, interflow, and deep groundwater circulation, as well as the water that recharges the springs. In order to derive unit kernel functions that represent a conservative system, moisture other than rapid groundwater recharge must be removed from the input series. Since a description of individual processes would necessitate a detailed understanding of the overall basin and spring hydrology, the excess precipitation is simply scaled so that the volume of the input in the deconvolution is equal to the volume of the output. This is done by scaling each member of the input series by a constant factor, the ratio of the response volume to the excess precipitation volume. The scaling assumes that the groundwater recharge that produces the spring storm response is a constant fraction of the excess precipitation. The scaling factor crudely lumps the complex interactions of surface flow, interflow, and deep groundwater circulation, and their effect on rapid groundwater recharge, into one factor. Because the scaling factor forces the volume of groundwater recharge to equal the volume of the storm response of the springs, it also eliminates the effect on the derived kernels of volume errors in other steps of the input and output calculations. Although any scaling method will

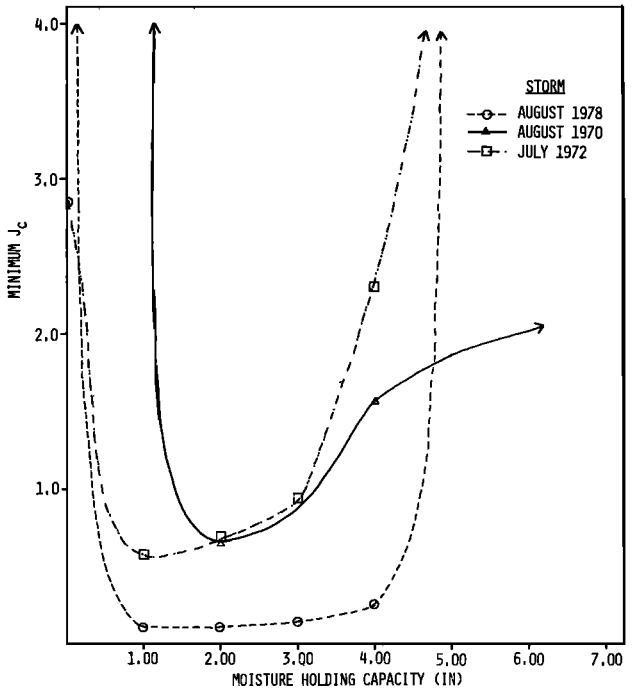

Fig. 12. Change in minimum predictive error with moisture-holding capacity for Big Spring responses to different storms.

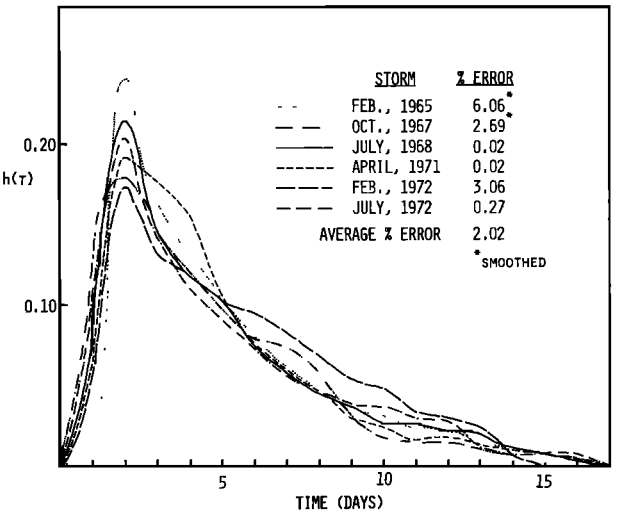

Fig. 13. Kernel functions for the response of Big Spring to different storms.

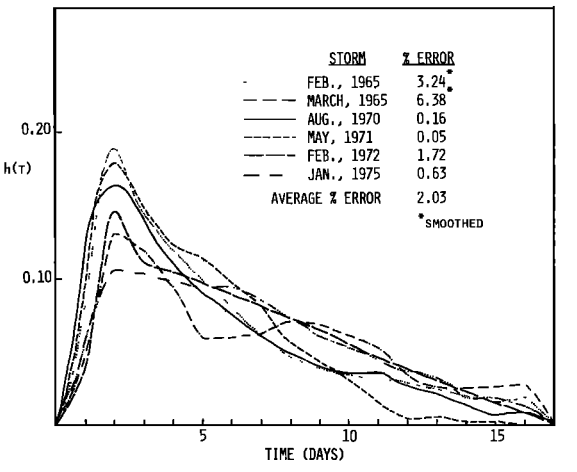

Fig. 14. Kernel functions for the response of Greer Spring to different storms.

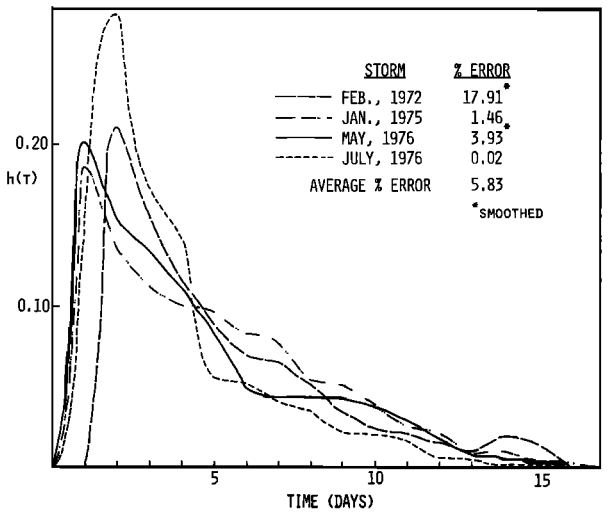

Fig. 15. Kernel functions for the response of Alley Spring to different storms.

remove the volume errors in the input and output calculations, a constant scaling factor maintains the relative distribution of the excess precipitation and the relative magnitudes of the kernel function ordinates. Therefore, this scaling method allows an evaluation of the sensitivity of the kernels to the hydrologic mechanisms that control distribution of the excess precipitation.

The magnitudes of the scaling factors computed for the Missouri springs vary significantly for different storms. This variability is not unexpected since anything that affects the volume of estimated excess precipitation or storm response will also affect the magnitude of the scaling factor. However, unless the magnitude of the scaling factor can be determined a priori, the computed kernels can be used only to reproduce the storm responses from which they were derived. They cannot be used to predict previously unknown storm responses.

Kernel Functions for Different Storms and Springs

Figures 13 to 16 show computed kernel functions for a number of different storms for Big, Greer, Alley, and Round springs. The kernel functions reproduce the storm responses from which they were derived with an average sum of absolute error of about 3%. Like surface flow unit hydrographs, the peak values of the kernel functions, the lag times of the peaks, and the accuracy with which the functions reproduce the system response differ between kernel functions.

The kernels for the two largest springs, Big Spring and Greer Spring, peak consistently at $t = 2$ days. The kernels for different storms are similar in shape, but Big Spring kernels have slightly greater peaks and vary less than Greer Spring kernels. The kernels for different storms for the smaller springs, Round and Alley springs, are more variable than those for the larger springs. The differences in the kernel functions for different storms for these springs are most apparent in the time to peak. Alley Spring kernel functions peak at either $t = 1$ or $t = 2$ days. Round Spring kernel functions peak at $t = 2$ or $t = 3$ days. This variability in the time to peak does not appear to be related to the storm magnitude or distribution, although it may result from inaccuracies in the moisture balance calculations or data measurements.

Average Kernel Functions

Single, average kernel functions were identified for each of the springs for multiple storms in order to extend the comparison of the derived kernel functions. These kernels were derived by identifying a single kernel from all of the input and output series for each spring, according to the relationship

$$y_{i,l} = \Delta t \sum_{j=0}^{i} (x_{j,l} h_{i-j}) + \varepsilon_{i,l} \qquad (10)$$

for $i = 0, 1, 2, \cdots, N$ and $l = 0, 1, 2, \cdots, K$, where $K + 1$ is the total number of input and output series, $y_{i,l}$ is the mean value of the output during interval i in the output series l, $x_{i,l}$ is the mean value of the input during interval i in the input series, and $\varepsilon_{i,l}$ represents the residual error.

The derived average kernel functions for each spring are shown in Figure 17. Identification of these kernels did not require smoothing. Unfortunately, because of the scaling factor in the moisture balance, the average kernels cannot be

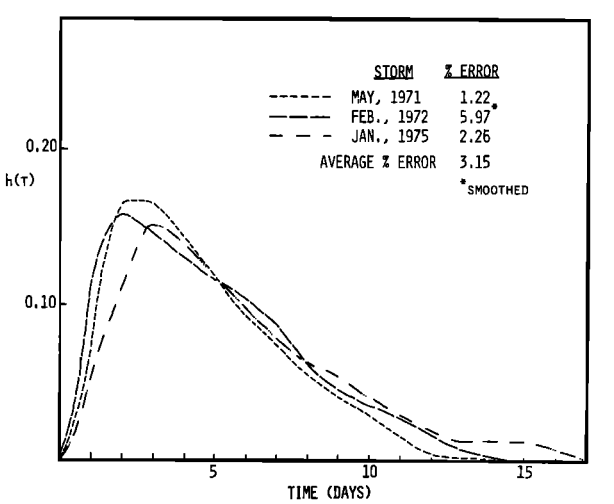

Fig. 16. Kernel functions for the response of Round Spring to different storms.

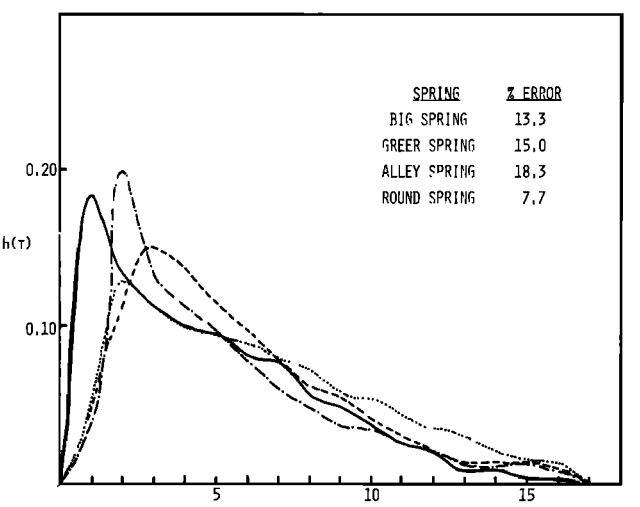

Fig. 17. Average kernel functions for different storms.

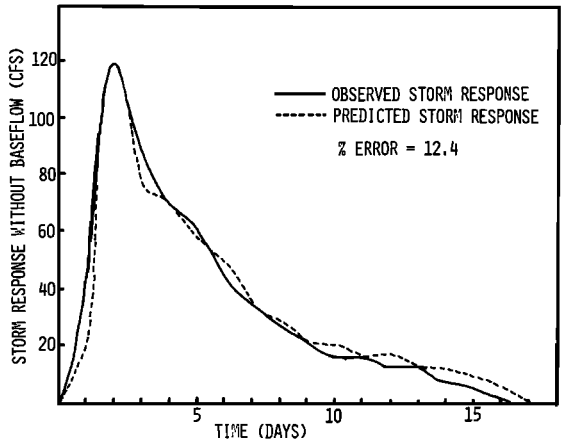

Fig. 18. Observed and predicted storm responses for July 1972 storm.

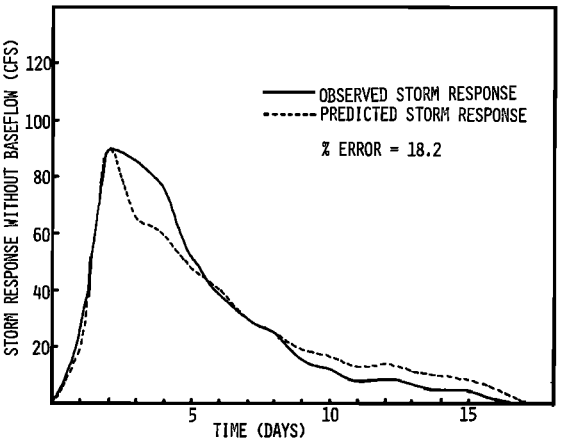

Fig. 19. Observed and predicted storm responses for April 1971 storm.

used to predict an unknown storm response and, therefore, cannot be completely validated. If the total volume of a storm response not used in the derivation of the average kernel is known, however, it is possible to predict the storm response by using the scaled input series and the average kernel function. This predicted response can then be compared with the actual storm response.

Figures 18 and 19 illustrate the range of error in the prediction of storm responses of Big Spring when using an average kernel function. In these examples an average kernel was derived from all of the input and output series except those of the storm used in the prediction. The identified kernels for the two cases were similar. Figure 18 is an example of one of the best storm response predictions. The average kernel identified without July 1972 storm data predicted the storm response with about 12% error. Figure 19 presents a poor prediction compared with the results of other storms. In this case the average kernel predicted the April 1971 storm response with about 18% error.

SUMMARY AND CONCLUSIONS

In summary, several observations and conclusions can be made about kernel functions for karst springs and the methodology presented here for the kernel identification:

1. Some of the major difficulties in identifying physically realistic kernel functions for karst springs can be overcome by using the deconvolution technique of *Neuman and de Marsily* [1976]. Successful kernel identification also requires estimation of an input series—groundwater recharge—and an output series—the spring flow storm response—from measured precipitation and spring flow data via the use of information about the hydrologic setting of the springs.

2. The derived kernels suggest a regularity in the response of individual springs to precipitation. Kernel functions identified for large karst springs, such as Big Spring or Greer Spring, from data for different isolated storms are similar in shape and time to peak. Average kernels for different springs vary, however, in both shape and time to peak. These average kernels, derived from multiple storm data without smoothing, predict spring flow responses to storms not used in the kernel derivation with less than 20% error.

3. The shape and predictive accuracy of derived kernels are sensitive to any assumptions or hydrologic factors that affect the relative distribution over time of the estimated input or output data. In general this sensitivity decreases, and the predictive accuracy of the kernels increases, for assumptions and ranges of values that are most physically reasonable.

4. Until the scaling factor in the moisture balance is better understood, the identified kernels can be used to predict only storm responses with known volumes. Since they cannot be used to predict previously unknown storm responses, the kernels presently cannot be validated. If the scaling factor can be better defined, kernel functions for karst springs may prove to be a useful tool for prediction of groundwater flow in karst aquifers.

Acknowledgments. The author is grateful to a number of people for their helpful criticisms and suggestions. S. Neuman and M. Diskin originally suggested the systems approach, and Neuman generously provided his program for data preparation. J. Vineyard and T. Aley supplied many useful details about the Missouri study area. The author is also grateful to I. Remson for his support and advice as a thesis advisor and to P. Switzer, J. Franzini, D. Freyberg, and N. Sitar for valuable discussions and comments. The research was partially supported by a grant from the Engineering Division of the National Science Foundation, ENG 7710160, and by a National Science Foundation Graduate Fellowship.

REFERENCES

Aley, T., *A Predictive Hydrologic Model for Evaluating the Effects of Land Use and Management on the Quantity and Quality of Water from Ozark Springs*, Ozark Underground Laboratory, Springfield, Mo., 1975.

Atkinson, T. C., D. I. Smith, R. J. Whitaker, and J. J. Lavis, Experiments in tracing underground waters in limestone, *J. Hydrol., 19*, 323–349, 1973.

Back, W., B. B. Hanshaw, T. E. Pyle, L. N. Plummer, and A. E. Weidie, Geochemical significance of groundwater discharge and carbonate solution to the formation of Caleta Xel Ha, Quintana Roo, Mexico, *Water Resour. Res., 15*(6), 1521–1535, 1979.

Blank, D. J., J. W. Delleur, and A. Giorgini, Oscillatory kernel functions in linear hydrologic models, *Water Resour. Res., 7*(5), 1102–1117, 1971.

Dreiss, S. J., An application of systems analysis to karst aquifers, Ph.D. thesis, Stanford Univ., Stanford, Cal., 1979.

Eagleson, P. S., R. Mejia-r, and F. March, Computation of optimum realizable unit hydrographs, *Water Resour. Res., 2*(4), 755–764, 1966.

Emsellem, Y., and G. de Marsily, Restitution automatique des permeabilities d'une nappe, le probleme inverse et al deconvolution, *Houille Blanche, 8*, 861–868, 1969.

Hanshaw, B. B., and W. Back, Determination of regional hydraulic conductivity through use of C^{14} dating of groundwater, *Mem. Int. Assoc. Hydrogeol., 10*(1), 195–198, 1974.

Klemt, W. B., T. R. Knowles, G. R. Elder, and T. W. Sieh, *Groundwater Resources and Model Applications for the Edwards (Bal-*

cones Fault Zone) Aquifer, Texas Water Development Board, Austin, Texas, 1975.
Knisel, W. G., Response of karst aquifers to recharge, *Hydrol. Pap. 60*, Colo. State Univ. Fort Collins, 1972.
Konikow, L. F., Preliminary digital model of groundwater flow in Madison Group, Powder River Basin, and adjacent areas, Wyoming, Montana, South Dakota, North Dakota, and Nebraska, *U. S. Geol. Surv. Open-File Rep. 63-77*, 1976.
Neuman, S. P., and G. de Marsily, Identification of linear systems response by parametric programming, *Water Resour. Res., 12*(2), 253–262, 1976.
Poitrinal, D., Qu'apporte la deconvolution a l'hydrogeologue?, *Mem. Int. Assoc. Hydrogeol., 10*(1), 238–241, 1974.
Poitrinal, D., and G. de Marsily, Relations du type entree-sortie en hydrogeologie procede d'identification de l'operateur, *Bull. Bur. Rech. Geol. Minière, Ser. 2, 3*(2), 119–135, 1973.
Shuster, E. T., and W. B. White, Source areas and climatic effects in carbonate groundwaters determined by saturation indices and carbon dioxide pressures, *Water Resour. Res., 8*(4), 1067–1073, 1972.
Thornthwaite, C. W., and J. R. Mather, Instructions and tables for computing potential evapotranspiration and the water balance, *Publ. Climatol.*, 10(3), 1957.

(Received July 31, 1980;
revised January 25, 1982;
accepted February 26, 1982.)